Title	Polydopamine nanoparticles for treatment of acute inflammation-induced injury
Authors	Zhao, He;Zeng, Zhandong;Liu, Lin;Chen, Jiawen;Zhou, Huiting;Huang, Lili;Huang, Jie;Xu, Hua;Xu, Yunyun;Chen, Zhengrong;Wu, Yi;Guo, Wanliang;Wang, Jiang Huai;Wang, Jian;Liu, Zhuang
Publication date	2018-03-13
Original Citation	Zhao, H., Zeng, Z., Liu, L., Chen, J., Zhou, H., Huang, L., Huang, J., Xu, H., Xu, Y., Chen, Z., Wu, Y., Guo, W., Wang, J. H., Wang, J. and Liu, Z. (2018) 'Polydopamine nanoparticles for treatment of acute inflammation-induced injury', Nanoscale. doi:10.1039/C8NR00838H
Type of publication	Article (peer-reviewed)
Link to publisher's version	10.1039/C8NR00838H
Rights	© 2018, the Authors. Published by the Royal Society of Chemistry. All rights reserved. This document is the accepted version of an article published in final form in Nanoscale. To access the final published work see http://dx.doi.org/10.1039/C8NR00838H
Download date	2024-11-11 01:13:31
Item downloaded from	https://hdl.handle.net/10468/5695

Nanoscale

Accepted Manuscript

This article can be cited before page numbers have been issued, to do this please use: H. Zhao, Z. Zeng, L. Liu, J. Chen, H. Zhou, L. Huang, J. Huang, H. Xu, Y. Xu, Z. Chen, Y. Wu, W. L. Guo, J. H. Wang, J. Wang and Z. Liu, *Nanoscale*, 2018, DOI: 10.1039/C8NR00838H.

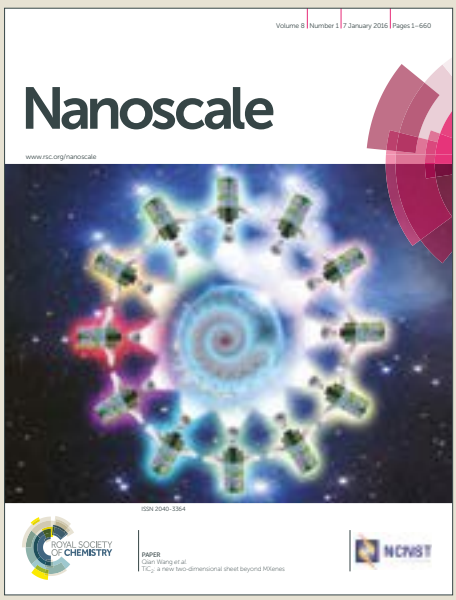

ROYAL SOCIETY OF CHEMISTRY

rsc.li/nanoscale

View Article Online
DOI: 10.1039/C8NR00838H

Polydopamine nanoparticles for treatment of acute inflammation-induced injury

He Zhao[1†], Zhandong Zeng[1†], Lin Liu[1†], Jiawen Chen[2], Huiting Zhou[1], Lili Huang[1], Jie Huang[1], Hua Xu[1], Yunyun Xu[1], Zhengrong Chen[1], Yi Wu[1], Wanliang Guo[1], Jiang Huai Wang[3], Jian Wang[1]*, Zhuang Liu[2]*

[1] Children's Hospital of Soochow University, Pediatric Research Institute of Soochow University, Suzhou, Jiangsu 215123, China

[2] Institute of Functional Nano & Soft Materials (FUNSOM), Jiangsu Key Laboratory for Carbon-Based Functional Materials & Devices, Soochow University, Suzhou, Jiangsu 215123, China

[3] Department of Academic Surgery, University College Cork, Cork University Hospital, Cork, Ireland

† These authors contributed equally to this work.

* Email: wj196312@vip.163.com, zliu@suda.edu.cn

Abstract

Nanotechnology-mediated anti-inflammatory therapy is emerging as a novel strategy for treatment of inflammation-induced injury. However, one of the main hurdles for these anti-inflammatory nano-drugs is their potential toxic side effects in vivo. Herein, we uncovered that polydopamine (PDA) nanoparticles with structure and chemical properties similar to melanin, a natural bio-polymer, displayed significant anti-inflammation therapeutic effect on acute inflammation-induced injury. PDA with enriched phenol groups functioned as a radical scavenger to eliminate reactive oxygen species (ROS) generated during inflammatory responses. As revealed by in vivo photoacoustic imaging with a H_2O_2-specific nanoprobe, PDA nanoparticles remarkably reduced intracellular ROS levels in murine macrophages challenged with either H_2O_2 or

View Article Online
DOI: 10.1039/C8NR00838H

lipopolysaccharide (LPS). The anti-inflammatory capacity of PDA nanoparticles was further demonstrated in murine models of both acute peritonitis and acute lung injury (ALI), where diminished ROS generation, reduced proinflammatory cytokines, attenuated neutrophil infiltration, and alleviated lung tissue damage were observed in PDA-treated mice after a single dose of PDA treatment. Our work therefore presents the great promise of PDA nanoparticles as a biocompatible nano-drug for anti-inflammation therapy to treat acute inflammation-induced injury.

Keywords: Polydopamine; Acute inflammation injury; Reactive oxygen species; Anti-inflammation therapy.

Introduction

Acute inflammatory response characterized by circulating neutrophils influx into the tissues and organs is a frequent event in the clinic, which causes tissue infection and damage in a short time period.[1-3] Among different types of acute inflammation, acute lung injury (ALI) and peritonitis are the simplest form of acute inflammatory responses. ALI is induced by the damage of alveolar epithelial cells and capillary endothelial cells and characterized with the dysregulated neutrophils sequestrated in the lung.[1, 4-8] These dysregulated neutrophils are capable of releasing proteases, cationic peptides and reactive oxygen species (ROS) to aggravate lung injury.[4, 9-12] Excessive ROS formation breaks the balance of endogenous anti-oxidative capacity and induces tissue damage and dysfunction. Therefore, prevention of the tissue damage by scavenging ROS could serve as a significant therapeutic option for treatment of acute inflammation-induced injury in the clinic.[13-15]

View Article Online
DOI: 10.1039/C8NR00838H

Polydopamine (PDA) derived from self-polymerization of dopamine shows many unique chemical properties and has attracted much attention in the area of nanomedicine.[16-22] PDA, a biocompatible and biodegradable polymer, has similar structure and chemical properties to that of melanin. With the versatile molecular adsorption ability, it has been found that PDA nanoparticles can be used for drug delivery, molecular imaging and cancer theranostics, as demonstrated in many previous studies.[17-19, 23-27] On the other hand, with a large amount of phenol groups on their surface, PDA nanoparticles show an excellent chelating ability to capture different types of metal ions such as radioisotope ions for nuclear imaging.[17, 23, 28-30] Moreover, those phenol groups also make PDA an excellent free radical scavenging agent.[16, 31] However, the applications of PDA nanoparticles as an anti-inflammatory agent to treat acute inflammation-induced injury including acute peritonitis and ALI have not yet been demonstrated to our best knowledge.

In this work, bare PDA nanoparticles were developed as anti-inflammatory nano-drug for treatment of acute inflammation-induced injury. At the in vitro level, it was discovered that PDA nanoparticles efficiently scavenged either H_2O_2- or LPS-induced cellular ROS. By utilizing our recently developed H_2O_2-responsive liposomal photoacoustic imaging nano-probe, we found that PDA nanoparticles were able to effectively suppress the in vivo inflammation process in an acute peritonitis model induced by LPS, as evidenced by the down-regulated ROS (e.g. H_2O_2) and pro-inflammatory cytokine levels after PDA treatment. Furthermore, using a murine model of ALI, we demonstrated that treatment with PDA nanoparticles ameliorated lung injury, with substantially diminished retention of neutrophils and lymphocytes in the lung and down-regulated levels of proinflammatory cytokines. Our results present an interesting anti-inflammation therapy platform by

View Article Online
DOI: 10.1039/C8NR00838H

utilizing the inherent biochemical properties of nanoparticles and suggest the potential application prospect of PDA nanoparticles as an anti-inflammatory nano-drug.

Results and Discussion

PDA nanoparticles were synthesized following a literature method **(Figure 1A)**.[16, 18] Transmission electron microscopy (TEM) image **(Figure 1B)** of the PDA sample showed that PDA nanoparticles were successfully formed with a uniform and mono-dispersed spherical structure. As shown in the TEM image, the average diameter of PDA nanoparticles was ~80 nm. Those as-made PDA nanoparticles were stable in water without any obvious aggregation, as revealed by dynamic light scattering measurement **(Figure 1C)**.

ROS are one of main reasons to cause various acute and chronic inflammatory diseases.[15, 32-36] Previous studies have demonstrated that H_2O_2 is one of the most common ROS types.[37-39] As such, we firstly examined the ROS scavenging activity of PDA nanoparticles toward H_2O_2. In our recent work, we fabricated a liposomal nanoprobe by encapsulating horseradish peroxidase (HRP) and its substrate, 2, 2'-azino-bis(3-ethylbenzothiazoline-6-sulfonic acid) (ABTS), into polyethylene glycol modified liposomes, and used such Lipo@HRP&ABTS as a H_2O_2-specific nanoprobe for in vivo photoacoustic (PA) imaging via the HRP-induced chromogenic reaction.[37] Therefore, using Lipo@HRP&ABTS as an indicator, the capability of PDA nanoparticles to scavenge H_2O_2 was evaluated. Firstly, PDA (0.01 mg/ml) was added into H_2O_2 (20 μM) solutions and incubated for various time periods. Afterwards, the Lipo@HRP&ABTS nanoprobe was added into those mixture solutions and incubated for 1 min under room temperature. As HRP in the presence of H_2O_2 would

View Article Online
DOI: 10.1039/C8NR00838H

convert colorless ABTS into its oxidized form with strong greenish color and the absorbance peak at ~730 nm, the absorbance spectrum changes of the reaction solution could be employed to determine the changes of H_2O_2 concentrations. Interestingly, we found that addition of PDA rapidly reduced the H_2O_2 concentration in the solution, as revealed by a decrease of absorbance from the Lipo@HRP&ABTS nanoprobe **(Figure 1D)**. Furthermore, an increase in PDA concentrations also resulted in a further decrease of H_2O_2 concentrations **(Figure 1E)**. Notably, the H_2O_2 scavenging activity of PDA increased as the solution pH increased from acidic to neutral values **(Supporting Information Figure S1B & 1C)**. Such a PDA-concentration-dependent H_2O_2 scavenging phenomenon could be vividly visualized by the obvious color change of PDA-treated H_2O_2 solutions in the presence of Lipo@HRP&ABTS nanoprobe **(Figure 1F)**. Besides, PA signals, which were originated from the 730 nm absorbance of Lipo@HRP&ABTS in response to H_2O_2, of the reaction solutions with different PDA concentrations were also detected **(Figure 1G)**. As the increase of PDA concentrations, the H_2O_2-specific PA signals from Lipo@HRP&ABTS showed dramatic decreases **(Figure 1G)**. It was noteworthy that even a rather low PDA concentration (0.01 mg/ml) was capable of inducing a significant decrease of the H_2O_2 concentration in the aqueous solution.

To understand the mechanism underlying the ability of PDA to scavenge H_2O_2, we examined whether PDA caused the decomposition of H_2O_2 by measuring O_2 production in the H_2O_2 solution after adding PDA nanoparticles. Without PDA, the rate of O_2 generation was quite slow as a result of self-decomposition of H_2O_2 **(Supporting Information Figure S1D)**. Interestingly, when PDA nanoparticles were added into the H_2O_2 solution, the O_2 production rate was greatly increased **(Supporting Information Figure S1D & 1E)**, suggesting the 'catalase-like' catalytic performance

View Article Online
DOI: 10.1039/C8NR00838H

of PDA to trigger the decomposition of H_2O_2 **(Supporting Information Figure S1F)**. Therefore, we propose that PDA nanoparticles could act as a H_2O_2 scavenger not only as a reducing agent to directly react with such ROS by redox reactions, but also as a catalyst to trigger decomposition of H_2O_2.

Next, the interactions between PDA nanoparticles and cells were studied at the in vitro level. After incubation with Raw 264.7 cells, PDA nanoparticles could be taken up into the cells **(Supporting Information Figure S2)**. The potential antioxidant and anti-inflammatory activities of PDA were then studied in vitro by a dye of 2,7-Dichloro-dihydrofluorescein diacetate (DCFH-DA), which is specifically responsive to intracellular ROS.[40] In our experiments, Raw 264.7 cells were pre-incubated with PDA for 6 h and then stimulated by H_2O_2 or LPS, the latter is a component from Gram-negative bacterial cell wall commonly used to stimulate oxidative stresses and induce inflammatory responses. As expected, the cellular ROS levels showed drastic increases upon exposure to either H_2O_2 or LPS. Interestingly, the ROS levels of cells pre-treated with PDA (PDA + H_2O_2 and PDA + LPS groups) were found to be significantly reduced, as revealed by both FACScan analysis and confocal fluorescence images of DCFH-DA stained cells **(Figure 2A-C&E and Supporting Information Figure S3A)**. Moreover, PDA treatment also effectively prevented H_2O_2-induced cytotoxicity to those cells **(Figure 2B-D)**. No obvious toxicity was observed after Raw 264.7 cells were incubated with different concentrations (up to 160 μg/ml) of PDA for 24 h **(Supporting Information Figure S3B)**. On the other hand, PDA nanoparticles could down-regulate the LPS-induced excretion of pro-inflammatory cytokine TNF-α by Raw 264.7 cells **(Supporting Information Figure S3C)**. Therefore, PDA nanoparticles showed significant antioxidant and

View Article Online
DOI: 10.1039/C8NR00838H

anti-inflammatory activities to reduce ROS production and protect cells from ROS-induced damage at the in vitro level.

Encouraged by the effective anti-inflammation ability of PDA in vitro, we then studied whether PDA nanoparticles could alleviate LPS-induced acute peritonitis in mice. Acute peritonitis was induced by intraperitoneal (i.p.) injection of LPS **(Figure 3A)** and mice were randomly divided into four groups (group 1-4): phosphate buffered solution (PBS) control group, PDA group, LPS group, and LPS + PDA group. PDA nanoparticles (10 mg/kg) were i.p. injected into the mice at 0.5 h after LPS injection in group 2 and group 4 **(Figure 3A)**. At different time points (24 h, 36 h and 48 h) post PDA injection, the mice were i.p. injected with Lipo@HRP&ABTS and imaged by a LAZR PA Imaging System.[37] LPS treatment resulted in strong photoacoustic signals in mouse abdomen owing to the inflammation-induced production of H_2O_2 **(Figure 3B&3C)**. Notably, administration of PDA remarkably reduced H_2O_2-associated photoacoustic signals in the mouse abdomen, suggesting largely decreased H_2O_2 levels in mice treated with PDA **(Figure 3B&3C)**. Furthermore, blood samples were collected at different time points for measurement of inflammation-related cytokines including TNF-α and IL-1β. It was found that serum levels of TNF-α in 'LPS + PDA' treatment group were significantly reduced at 24 h, 36 h, and 48 h post PDA treatment compared to LPS group **(Figure 3D)**, whereas serum levels of IL-1β also showed the same decreasing trend at 36 h post PDA treatment **(Supporting Information Figure S4)**. Therefore, both PA imaging and serum cytokine data indicate that the inflammatory response initiated during LPS-induced acute peritonitis is greatly attenuated by treatment with PDA nanoparticles.

ALI is even more common than acute peritonitis in the clinic. In our experiments, ALI model

View Article Online
DOI: 10.1039/C8NR00838H

was established by intranasal instillation of LPS into mice **(Figure 4A)**. Thereafter, these mice were intravenously (i.v.) injected or intranasally (n.a.) dropped with PDA nanoparticles **(Figure 4A)** at the different time points post LPS stimulation. The biodistribution analysis based on ^{131}I-labeled PDA nanoparticles revealed that PDA nanoparticles predominantly accumulated in the lung at 24 h post PDA injection or dripping **(Figure 4B & C)**. In comparison with i.v. injection, the n.a. dripping method led to a much higher accumulation of PDA nanoparticles in the lung with lower retention in other organs such as liver and spleen **(Figure 4B & C)**.

Based on the biodistribution analysis, in order to seek the best method and timing of PDA administration to treat ALI, we further studied the therapeutic effect of PDA nanoparticles under either n.a. dripping or i.v. injection. Firstly, the administration time of PDA nanoparticles was assessed. It was uncovered that the earlier PDA nanoparticles were administrated for ALI treatment, the better therapeutic effect could be, no matter n.a. dripping or i.v. injection **(Figure 4D - G)**. Notably, when PDA nanoparticles were administrated within 0.5 h after ALI was initiated, lung myeloperoxidase (MPO) activity, total leukocyte numbers, total protein concentrations, and total neutrophil counts were all significantly down-regulated, suggesting the remarkable therapeutic effect of PDA nanoparticles to treat ALI **(Figure 4D - G)**. Thereafter, the therapeutic efficacy between n.a. dripping and i.v. injection was compared. It is well documented that dysregulated leukocytes, especially neutrophils, play an important role in aggravating ALI.[4, 9] Interestingly, compared to i.v. injection, n.a. dripping of PDA nanoparticles resulted in a more markedly decrease in total protein concentrations, especially the total leukocyte and neutrophil numbers **(Figure 4E - G)**. Hematoxylin and eosin (H&E) staining of lung tissues collected at 24 h also demonstrated that n.a. administration

View Article Online
DOI: 10.1039/C8NR00838H

of PDA offered better therapeutic outcome compared to that achieved by the i.v. injection route for ALI treatment **(Supporting Information Figure S5)**. Therefore, we chose intranasal dripping at 0.5 h post initiation of ALI to evaluate the therapeutic effect of PDA nanoparticles in details.

Based on above findings, the time-dependent efficacy of PDA nanoparticles to ameliorate LPS-induced ALI was further evaluated. ALI model was induced by LPS **(Figure 5A)** and mice were randomly divided into four groups: PBS group, PDA group, LPS group, and LPS + PDA group. Mice were n.a. dropped by PDA (10 mg/kg) at 0.5 h post LPS inhalation. Administration of PDA markedly attenuated proinflammatory cytokines IL-6, TNF-α, and CXCL-2 in BALF of LPS-induced ALI mice at all tested time points, but did not affect these cytokine levels in normal healthy mice **(Figure 5B, 5C & 5D)**. Meanwhile, PDA significantly reduced total leukocytes and neutrophils counts, lung MPO activity, and total protein levels in BALF of LPS-induced ALI mice **(Figure 5E - 5H)**.

Histological examination of the lung tissues was further conducted to directly evaluate the therapeutic outcome. In the lung of the 'LPS group', epithelioid cell proliferation and infiltration of inflammatory cells (mainly neutrophils) were observed **(Figure 6)**. By contrast, administration of PDA could effectively ameliorate lung morphological changes and significantly reduce neutrophil infiltration as observed in the 'LPS + PDA group' **(Figure 6)**. These results indicated that PDA could observably alleviate LPS-induced ALI in vivo, promising the ALI therapy.

Conclusion

In summary, PDA nanoparticles were developed for treatment of acute inflammation-induced injury, as demonstrated in both murine acute peritonitis and ALI models. The characteristics of PDA

View Article Online
DOI: 10.1039/C8NR00838H

nanoparticles in eliminating ROS were carefully studied for understanding the antioxidation mechanisms. We uncover that PDA nanoparticles could act as a ROS scavenger not only as a reducing agent to directly react with ROS, but also as a catalyst to trigger decomposition of H_2O_2. At the cellular level, PDA nanoparticles strongly down-regulated intracellular ROS levels in response to inflammatory stimulation. Consistent with the anti-oxidative and anti-inflammatory properties of PDA nanoparticles, in vivo ROS generation during acute peritonitis was substantially relieved in mice treated with PDA, as confirmed by photoacoustic imaging using a H_2O_2-specific nanoprobe. The anti-inflammation activity of PDA nanoparticles was further evaluated in the ALI model. After a single dose of PDA treatment, PDA nanoparticles markedly improved ALI, with significantly reduced neutrophil infiltration, decreased BALF protein concentrations, and improved lung morphological alterations. Therefore, an interesting therapeutic nano-drug based on PDA nanoparticles is developed in this work, useful for not only protecting the tissue from ROS injury, but also improving the behavior of dysregulated neutrophils to ameliorate acute inflammation. Such a strategy may significantly improve the clinical outcomes for not only ALI, but also other inflammatory diseases with dysregulated neutrophils, such as acute respiratory distress syndrome, acute gout of liver encephalopathy and epilepsy. This study thus presents the great promising of applying nanomedicine for anti-inflammation therapy.

Materials and methods

Materials. Dopamine hydrochloride, 2,2'-Azino-bis(3-ethylbenzthiazoline-6-sulfonic acid) (ABTS), horseradish peroxidase (HRP), lipopolysaccharide (LPS) and 2',7'-Dichlorofluorescin

View Article Online
DOI: 10.1039/C8NR00838H

diacetate (DCFH-DA) were purchased from Sigma-Aldrich and used as received. Hydrogen peroxide (H_2O_2) was purchased from China National Pharmaceutical Group Corporation. Raw 264.7 macrophage cells were obtained from American Type Culture Collection (ATCC). DMEM culture medium was obtained from Thermo Fisher Scientific Inc. Female Balb/c mice were purchased from Nanjing Peng Sheng Biological Technology Co. Ltd.

Preparation of PDA nanoparticles. PDA nanoparticles were synthesized according to a method previously reported.[16, 18] Briefly, 90 mg dopamine hydrochloride was dissolved in 45 ml deionized water, into which 0.38 ml of 1 M NaOH solution was added. After self- polymerization for 2 h, PDA nanoparticles were obtained by centrifugation (14800 rpm) and washed with deionized water for several times.

Characterization. The morphology of PDA was characterized with FEI Tecnai F20 transmission electron microscopy. UV–Vis–NIR absorption spectra were measured by a GENESYS 10S UV–Vis spectrophotometer. The hydrodynamic light scattering (DLS) was acquired by a Zetasizer Nano Z (Malvern).

Catalysis of H_2O_2 by PDA nanoparticles. The O_2 release in the H_2O_2 solution with or without PDA (0.01 mg/ml) was measured by a dissolved oxygen meter (Rex, JPBJ-608, China). The decomposition of H_2O_2 (100 μM) was determined by an ABTS assay. A liposomal H_2O_2-specific nanoprobe, Lipo@HRP&ABTS, was synthesized according to our recently reported protocol.[37] PDA

View Article Online
DOI: 10.1039/C8NR00838H

solutions with different concentrations (0.01, 0.02, 0.03 mg/ml) were mixed with H_2O_2 for 5-10 minutes, and then incubated with Lipo@HRP&ABTS solution. The absorbance of the mixture after reaction was measured using a UV–Vis spectrophotometer.

Cell uptake of PDA nanoparticles. To test the cell uptake of nanoparticles, Raw 264.7 cells, a murine macrophage cell line, were incubated with FITC labeled PDA nanoparticles (PDA-FITC, 80 μg/ml) for various periods of time. Afterwards, the cells were washed by PBS three times and imaged under a confocal fluorescence microscope (OLYMPUS, IX73).

Intracellular ROS scavenging by PDA nanoparticles. To evaluate the ROS scavenging in vitro, Raw 264.7 cells were seeded in 24-well plates and incubated with PDA (80 μg/ml) for 6 hours before adding H_2O_2 (100 and 200 μM). After 30 minutes of exposure to H_2O_2, the cells were washed by PBS twice and then incubated with DCFH-DA. Flow cytometry (ESP Elite, Beckman Coulter, Fullerton, CA, USA) was used to test the levels of ROS in the cells by detecting the mean fluorescence intensity (MFI) of DCFH-DA fluorescence. For cell viability assay, Raw 264.7 cells were seeded in a 96-well plate and mixed with PDA (80 μg/ml), with or without adding H_2O_2. After 24 hours incubation, the cells were washed and the cell viability was determined by the cell counting kit (CCK-8) assay. For the anti-inflammatory study of PDA in vitro, PDA nanoparticles (80 μg/ml) were incubated with Raw 264.7 cells for 6 hours. Then, the cells were treated with LPS. Intracellular ROS levels were assessed using DCFH-DA staining by flow cytometry. Additionally, DCFH-DA fluorescence in the cells was visualized by a confocal fluorescence microscope (OLYMPUS, IX73).

View Article Online
DOI: 10.1039/C8NR00838H

Peritoneal inflammation amelioration for PA imaging. All animal procedures were performed in accordance with the Guidelines for Care and Use of Laboratory Animals of Soochow University and approved by the Animal Ethics Committee of Soochow University. Female BALB/c mice (8-10 weeks) were purchased from Nanjing Peng Sheng Biological Technology Co Ltd and randomly divided into four groups: phosphate buffered solution (PBS) control, PDA control, LPS-treated group, and PDA + LPS-treated group (4 mice per group), which were intraperitoneally (i.p.) injected with PBS (0.1 ml), PDA (10 mg/kg), LPS (5 mg/kg), and PDA (10 mg/kg) + LPS (5 mg/kg), respectively. At different time points (24 hours, 36 hours, 48 hours) after injection, the mice were i.p. injected with H_2O_2-responsive probe Lipo@HRP&ABTS for photoacoustic (PA) imaging of peritoneal inflammation by in vivo detection of H_2O_2.[37] All images on the abdomen were assessed using a Vevo LAZR Imaging System (FujiFilm VisualSonics Inc.). Besides, serum samples in all groups were collected from the mouse eyes. And serum cytokines (TNF-α, IL-1β) were analyzed with ELISA kits (eBioscience, San Diego, CA, USA), according to the manufacturer's instructions. All animal studies were approved by Soochow University Laboratory Animal Center.

Biodistribution of PDA nanoparticles. ^{131}I-labeled PDA was prepared according to the previous reports.[23] For intravenous route, female BALB/c mice were intravenously (i.v.) injected with ^{131}I-PDA (PDA: 10 mg/kg, 200 μCi of ^{131}I). After 24 hours post injection, major organs including liver, spleen, kidney, heart, lung, skin, muscle, bone, stomach and small intestine were collected and measured by the gamma counter (Science and Technology Institute of China in Jia Branch Innovation

View Article Online
DOI: 10.1039/C8NR00838H

Co., Ltd.).

LPS-induced ALI. Female BALB/c mice (8-10 weeks) were used for those experiments. The ALI model was induced with n.a. instillation of LPS, according to the standard method previously reported.[41-42] At 24, 36 and 48 hours after LPS inhalation, the lung tissues and bronchoalveolar lavage fluid (BALF) were collected after three times lavages and stored at – 80 ^{o}C. BALF samples were directly used for analyses without any additional treatment.

Measurement of lung MPO activity. The groups were the same as before: PBS group, PDA control, LPS-treated group, and PDA + LPS-treated group (4 mice per group). Right lung tissues of the mice were homogenized and centrifuged. The supernatant solution was used to analyze and quantify lung MPO activity with the MPO assay kit (Nanjing Jiancheng Bioengineering Institute) according to the vendors' instructions.

Assessment of leukocyte number, total protein concentration, inflammatory cytokines and chemokine in BALF. After lung lavage for three times, BALF was obtained.[41] A standard haemocytometer and Wright-Giemsa staining assay was used to assess the counts of total and differentiated leukocytes. A BCA protein assay kit (Piece, Rockford, IL, USA) was used to measure the total protein concentration in BALF. The levels of inflammatory cytokines (TNF-α, IL-6 and IL-1β) and chemokine (CXCL2) in BALF were determined by ELISA (eBioscience, San Diego, CA, USA), according to the supplier' instructions.

View Article Online
DOI: 10.1039/C8NR00838H

Lung histological examination. Left lung tissues of the mouse were harvested and fixation in 4 % paraformaldehyde for hematoxylin and eosin (H&E) staining at 24 hours, 36 hours and 48 hours after LPS instillation. Lung slices were observed for evaluating morphological changes by a digital microscope (Leica QWin).

Statistical analysis. The statistical analyses were performed by using Student's t-test for the p value (* $p < 0.05$, ** $p < 0.01$, *** $p < 0.001$). The values were expressed as mean ± standard deviation (SD) for control and experimental samples.

Acknowledgements

This work was partially supported by the National Basic Research Programs of China (973 Program)(2016YFA0201200), the National Natural Science Foundation of China (81602181, 81501703, 81500733, 81502500, 81420108022, 81272143, 51525203, 31300824, 81701948), the Natural Science Foundation of Jiangsu Province (BK20150292, 20150293, 20150294), the Suzhou Municipal Science and Technology Project (SYS201565, SYS201759), Key Laboratory of Suzhou (SZS201307), Suzhou Clinical Medicine Center (Szzxj201505), a Jiangsu Natural Science Fund for Distinguished Young Scholars (BK20130005), Collaborative Innovation Center of Suzhou Nano Science and Technology, and a Project Funded by the Priority Academic Program Development (PAPD) of Jiangsu Higher Education Institutions.

View Article Online
DOI: 10.1039/C8NR00838H

Conflict of interest

The authors declare that they have no competing interests.

References

1. Wang, J.; Liu, Y.-T.; Xiao, L.; Zhu, L.; Wang, Q.; Yan, T., Anti-inflammatory effects of apigenin in lipopolysaccharide-induced inflammatory in acute lung injury by suppressing COX-2 and NF-kB pathway. *Inflammation* **2014,** *37* (6), 2085-2090.

2. Jiang, W.; Luo, F.; Lu, Q.; Liu, J.; Li, P.; Wang, X.; Fu, Y.; Hao, K.; Yan, T.; Ding, X., The protective effect of Trillin LPS-induced acute lung injury by the regulations of inflammation and oxidative state. *Chemico-biological interactions* **2016,** *243*, 127-34.

3. Levy, B. D.; Serhan, C. N., Resolution of acute inflammation in the lung. *Annual review of physiology* **2014,** *76*, 467-492.

4. Liu, Y.-L.; Liu, Y.-J.; Liu, Y.; Li, X.-S.; Liu, S.-H.; Pan, Y.-G.; Zhang, J.; Liu, Q.; Hao, Y.-Y., Hydroxysafflor yellow A ameliorates lipopolysaccharide-induced acute lung injury in mice via modulating toll-like receptor 4 signaling pathways. *International immunopharmacology* **2014,** *23* (2), 649-657.

5. Sayah, D. M.; Mallavia, B.; Liu, F.; Ortiz-Muñoz, G.; Caudrillier, A.; DerHovanessian, A.; Ross, D. J.; Lynch III, J. P.; Saggar, R.; Ardehali, A., Neutrophil extracellular traps are pathogenic in primary graft dysfunction after lung transplantation. *American journal of respiratory and critical care medicine* **2015,** *191* (4), 455-463.

6. Grailer, J. J.; Kalbitz, M.; Zetoune, F. S.; Ward, P. A., Persistent neutrophil dysfunction and suppression of acute lung injury in mice following cecal ligation and puncture sepsis. *Journal of innate immunity* **2014,** *6* (5), 695-705.

7. Wang, J. H., Blocking of Kinin B1 Receptor: A Promising Way for the Treatment of Acute Lung Injury. *Critical care medicine* **2015,** *43* (11), 2520-2522.

8. Zhan, Y.; Zeng, W.; Jiang, G.; Wang, Q.; Shi, X.; Zhou, Z.; Deng, H.; Du, Y., Construction of lysozyme exfoliated rectorite-based electrospun nanofibrous membranes for bacterial inhibition. *Journal of Applied Polymer Science* **2015,** *132* (8), n/a-n/a.

9. Pratheeshkumar, P.; Son, Y.-O.; Divya, S. P.; Roy, R. V.; Hitron, J. A.; Wang, L.; Kim, D.; Dai, J.; Asha, P.; Zhang, Z., Luteolin inhibits Cr (VI)-induced malignant cell transformation of human lung epithelial cells by targeting ROS mediated multiple cell signaling pathways. *Toxicology and applied pharmacology* **2014,** *281* (2), 230-241.

10. Matsebatlela, T. M.; Anderson, A. L.; Gallicchio, V. S.; Elford, H.; Rice, C. D., 3, 4-Dihydroxy-benzohydroxamic acid (Didox) suppresses pro-inflammatory profiles and oxidative stress in TLR4-activated RAW264. 7 murine macrophages. *Chemico-biological interactions* **2015,** *233*, 95-105.

11. Lomas-Neira, J.; Venet, F.; Chung, C.-S.; Thakkar, R.; Heffernan, D.; Ayala, A., Neutrophil–endothelial interactions mediate angiopoietin-2–associated pulmonary endothelial cell dysfunction in

View Article Online
DOI: 10.1039/C8NR00838H

indirect acute lung injury in mice. *American journal of respiratory cell and molecular biology* **2014,** *50* (1), 193-200.

12. Ikoba, U.; Peng, H.; Li, H.; Miller, C.; Yu, C.; Wang, Q., Nanocarriers in therapy of infectious and inflammatory diseases. *Nanoscale* **2015,** *7* (10), 4291-4305.

13. Zhang, W.; Hu, S.; Yin, J.-J.; He, W.; Lu, W.; Ma, M.; Gu, N.; Zhang, Y., Prussian blue nanoparticles as multienzyme mimetics and reactive oxygen species scavengers. *Journal of the American Chemical Society* **2016,** *138* (18), 5860-5865.

14. Huang, Y.; Liu, Z.; Liu, C.; Ju, E.; Zhang, Y.; Ren, J.; Qu, X., Self‐Assembly of Multi‐nanozymes to Mimic an Intracellular Antioxidant Defense System. *Angewandte Chemie International Edition* **2016,** *55* (23), 6646-6650.

15. Liu, Y.; Ai, K.; Ji, X.; Askhatova, D.; Du, R.; Lu, L.; Shi, J., Comprehensive Insights into the Multi-Antioxidative Mechanisms of Melanin Nanoparticles and Their Application To Protect Brain from Injury in Ischemic Stroke. *J Am Chem Soc* **2017,** *139* (2), 856-862.

16. Ju, K. Y.; Lee, Y.; Lee, S.; Park, S. B.; Lee, J. K., Bioinspired polymerization of dopamine to generate melanin-like nanoparticles having an excellent free-radical-scavenging property. *Biomacromolecules* **2011,** *12* (3), 625-32.

17. Dong, Z.; Gong, H.; Gao, M.; Zhu, W.; Sun, X.; Feng, L.; Fu, T.; Li, Y.; Liu, Z., Polydopamine Nanoparticles as a Versatile Molecular Loading Platform to Enable Imaging-guided Cancer Combination Therapy. *Theranostics* **2016,** *6* (7), 1031-42.

18. Zhao, H.; Chao, Y.; Liu, J.; Huang, J.; Pan, J.; Guo, W.; Wu, J.; Sheng, M.; Yang, K.; Wang, J., Polydopamine coated single-walled carbon nanotubes as a versatile platform with radionuclide labeling for multimodal tumor imaging and therapy. *Theranostics* **2016,** *6* (11), 1833.

19. Liu, Y.; Ai, K.; Lu, L., Polydopamine and its derivative materials: synthesis and promising applications in energy, environmental, and biomedical fields. *Chemical reviews* **2014,** *114* (9), 5057-5115.

20. Peng, H.; Wang, C.; Xu, X.; Yu, C.; Wang, Q., An intestinal Trojan horse for gene delivery. *Nanoscale* **2015,** *7* (10), 4354-4360.

21. Li, W.; Li, X.; Wang, Q.; Pan, Y.; Wang, T.; Wang, H.; Song, R.; Deng, H., Antibacterial activity of nanofibrous mats coated with lysozyme-layered silicate composites via electrospraying. *Carbohydrate Polymers* **2014,** *99* (Supplement C), 218-225.

22. Chen, W.; Shen, X.; Hu, Y.; Xu, K.; Ran, Q.; Yu, Y.; Dai, L.; Yuan, Z.; Huang, L.; Shen, T.; Cai, K., Surface functionalization of titanium implants with chitosan-catechol conjugate for suppression of ROS-induced cells damage and improvement of osteogenesis. *Biomaterials* **2017,** *114*, 82-96.

23. Zhong, X.; Yang, K.; Dong, Z.; Yi, X.; Wang, Y.; Ge, C.; Zhao, Y.; Liu, Z., Polydopamine as a biocompatible multifunctional nanocarrier for combined radioisotope therapy and chemotherapy of cancer. *Advanced Functional Materials* **2015,** *25* (47), 7327-7336.

24. Lin, L.-S.; Cong, Z.-X.; Cao, J.-B.; Ke, K.-M.; Peng, Q.-L.; Gao, J.; Yang, H.-H.; Liu, G.; Chen, X., Multifunctional Fe3O4@ polydopamine core–shell nanocomposites for intracellular mRNA detection and imaging-guided photothermal therapy. *ACS nano* **2014,** *8* (4), 3876-3883.

25. Chen, Y.; Ai, K.; Liu, J.; Ren, X.; Jiang, C.; Lu, L., Polydopamine-based coordination nanocomplex for T 1/T 2 dual mode magnetic resonance imaging-guided chemo-photothermal

View Article Online
DOI: 10.1039/C8NR00838H

synergistic therapy. *Biomaterials* **2016,** *77*, 198-206.

26. Wang, Q.; Zhang, R.; Lu, M.; You, G.; Wang, Y.; Chen, G.; Zhao, C.; Wang, Z.; Song, X.; Wu, Y., Bioinspired Polydopamine-Coated Hemoglobin as Potential Oxygen Carrier with Antioxidant Properties. *Biomacromolecules* **2017,** *18* (4), 1333-1341.

27. Xing, Y.; Zhang, J.; Chen, F.; Liu, J.; Cai, K., Mesoporous polydopamine nanoparticles with co-delivery function for overcoming multidrug resistance via synergistic chemo-photothermal therapy. *Nanoscale* **2017,** *9* (25), 8781-8790.

28. Zeng, Y.; Zhang, D.; Wu, M.; Liu, Y.; Zhang, X.; Li, L.; Li, Z.; Han, X.; Wei, X.; Liu, X., Lipid-AuNPs@ PDA nanohybrid for MRI/CT imaging and photothermal therapy of hepatocellular carcinoma. *ACS applied materials & interfaces* **2014,** *6* (16), 14266-14277.

29. Dai, Y.; Yang, D.; Yu, D.; Cao, C.; Wang, Q.; Xie, S.; Shen, L.; Feng, W.; Li, F., Mussel-Inspired Polydopamine Coated Lanthanide Nanoparticles for NIR-II/CT Dual Imaging and Photothermal Therapy. *ACS Applied Materials & Interfaces* **2017**.

30. Yao, S.; Li, X.; Liu, J.; Sun, Y.; Wang, Z.; Jiang, Y., Maximized nanodrug-loaded mesenchymal stem cells by a dual drug-loaded mode for the systemic treatment of metastatic lung cancer. *Drug Delivery* **2017,** *24* (1), 1372-1383.

31. Xiong, S. Q.; Wang, Y.; Zhu, J.; Hu, Z. M.; Yu, J. R. In *Polydopamine Nanoparticle for Poly (N-Isopropylacrylamide)-Based Nanocomposite Hydrogel with Good Free-Radical-Scavenging Property*, Materials Science Forum, Trans Tech Publications Ltd.: 2016; p 94.

32. Sedlak, T. W.; Saleh, M.; Higginson, D. S.; Paul, B. D.; Juluri, K. R.; Snyder, S. H., Bilirubin and glutathione have complementary antioxidant and cytoprotective roles. *Proceedings of the national academy of sciences* **2009,** *106* (13), 5171-5176.

33. Nathan, C.; Cunningham-Bussel, A., Beyond oxidative stress: an immunologist's guide to reactive oxygen species. *Nature Reviews. Immunology* **2013,** *13* (5), 349.

34. Barnham, K. J.; Masters, C. L.; Bush, A. I., Neurodegenerative diseases and oxidative stress. *Nature reviews. Drug discovery* **2004,** *3* (3), 205.

35. Ju, E.; Liu, Z.; Du, Y.; Tao, Y.; Ren, J.; Qu, X., Heterogeneous assembled nanocomplexes for ratiometric detection of highly reactive oxygen species in vitro and in vivo. *ACS nano* **2014,** *8* (6), 6014-6023.

36. Chia, S. L.; Tay, C. Y.; Setyawati, M. I.; Leong, D. T., Biomimicry 3D gastrointestinal spheroid platform for the assessment of toxicity and inflammatory effects of zinc oxide nanoparticles. *Small* **2015,** *11* (6), 702-712.

37. Chen, Q.; Liang, C.; Sun, X.; Chen, J.; Yang, Z.; Zhao, H.; Feng, L.; Liu, Z., H2O2-responsive liposomal nanoprobe for photoacoustic inflammation imaging and tumor theranostics via in vivo chromogenic assay. *Proceedings of the National Academy of Sciences* **2017,** *114* (21), 5343-5348.

38. Lee, Y.; Kim, H.; Kang, S.; Lee, J.; Park, J.; Jon, S., Bilirubin Nanoparticles as a Nanomedicine for Anti-inflammation Therapy. *Angewandte Chemie* **2016,** *55* (26), 7460-3.

39. Zhang, Y.; Wang, L.; Sun, Y.; Zhu, Y.; Zhong, Z.; Shi, J.; Fan, C.; Huang, Q., Conjugation of dexamethasone to C60 for the design of an anti-inflammatory nanomedicine with reduced cellular apoptosis. *ACS applied materials & interfaces* **2013,** *5* (11), 5291-5297.

40. Su, H.-L.; Chou, C.-C.; Hung, D.-J.; Lin, S.-H.; Pao, I.-C.; Lin, J.-H.; Huang, F.-L.; Dong,

View Article Online
DOI: 10.1039/C8NR00838H

R.-X.; Lin, J.-J., The disruption of bacterial membrane integrity through ROS generation induced by nanohybrids of silver and clay. *Biomaterials* **2009,** *30* (30), 5979-5987.

41. Li, Y.; Huang, J.; Foley, N. M.; Xu, Y.; Li, Y. P.; Pan, J.; Redmond, H. P.; Wang, J. H.; Wang, J., B7H3 ameliorates LPS-induced acute lung injury via attenuation of neutrophil migration and infiltration. *Scientific reports* **2016,** *6*, 31284.

42. Xu, Y.; Xiang, J.; Zhao, H.; Liang, H.; Huang, J.; Li, Y.; Pan, J.; Zhou, H.; Zhang, X.; Wang, J. H., Human amniotic fluid stem cells labeled with up-conversion nanoparticles for imaging-monitored repairing of acute lung injury. *Biomaterials* **2016,** *100*, 91-100.

View Article Online
DOI: 10.1039/C8NR00838H

TOC Figure

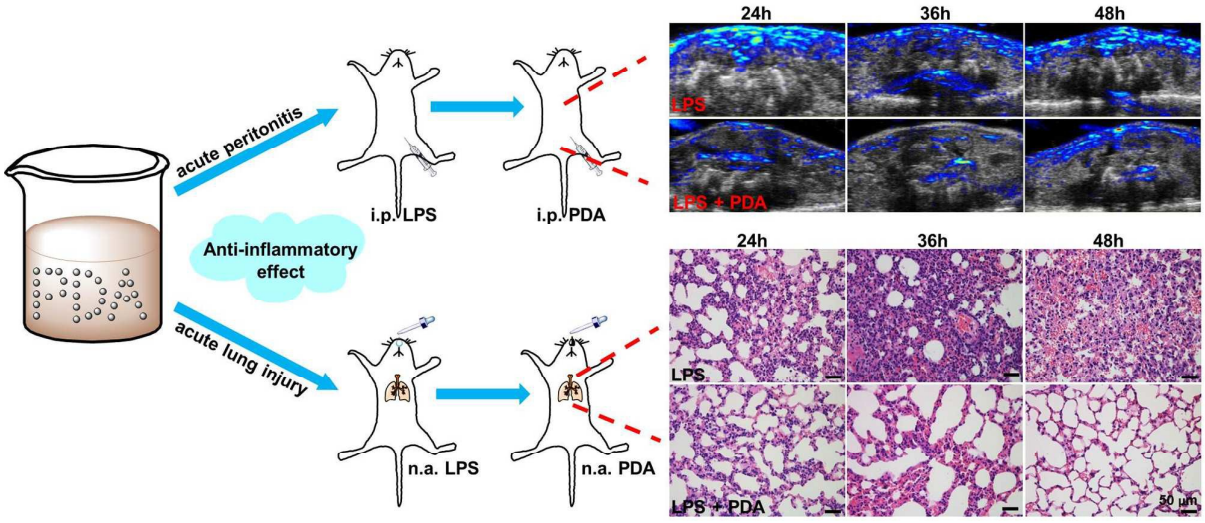

View Article Online
DOI: 10.1039/C8NR00838H

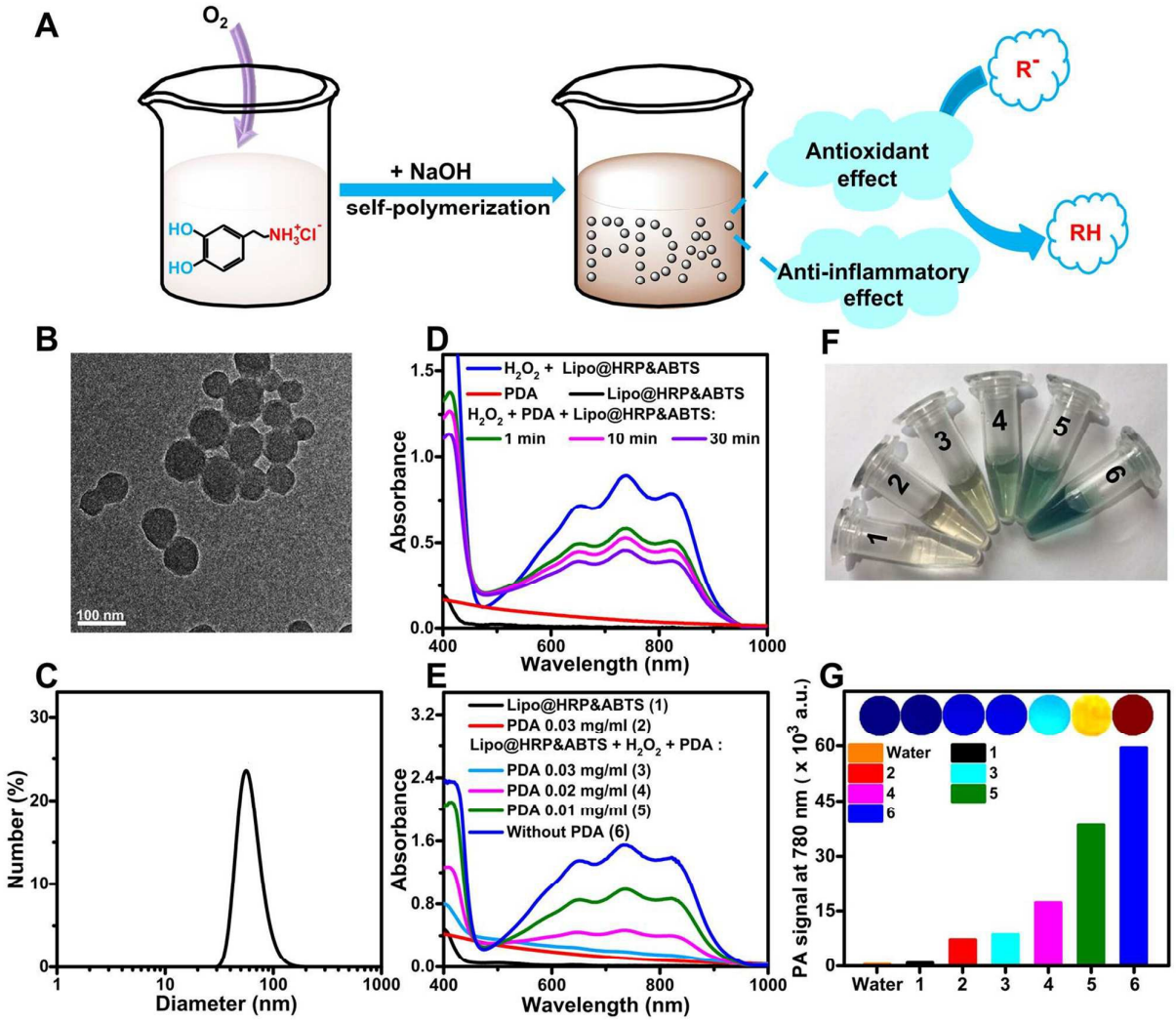

Figure 1. Preparation and ROS elimination characterization of PDA. (A) A schematic illustration for the synthesis of PDA and effect of PDA for protecting the tissue from oxidative and inflammatory injury. (B) TEM image of PDA nanoparticles. (C) Hydrodynamic diameters of PDA nanoparticles in water. (D) UV-Vis-NIR absorbance spectra changes of the reaction solutions measured at different time point (i.e. 1 min, 10 min, 30 min) after H_2O_2 (20 μM) was incubated with PDA (0.01 mg/ml). The absorbance was originated from the Lipo@HRP&ABTS probe in the presence of H_2O_2. (E&F) UV-Vis-NIR absorbance spectra (E) and the photo (F) of the mixture solutions, including free Lipo@HRP&ABTS, free PDA, and Lipo@HRP&ABTS mixed with H_2O_2 (25 μM) pre-incubated with different concentrations of PDA for 10 min. (G) PA images (up) and PA signal intensities at 780 nm (bottom) of the mixture solutions. 1: Lipo@HRP&ABTS solution. 2: PDA (0.03 mg/ml) solution. 3 - 6: the mixture solutions of Lipo@HRP&ABTS, H_2O_2 (25 μM) and PDA at different concentrations (0.03, 0.02, 0.01 and 0.00 mg/ml).

View Article Online
DOI: 10.1039/C8NR00838H

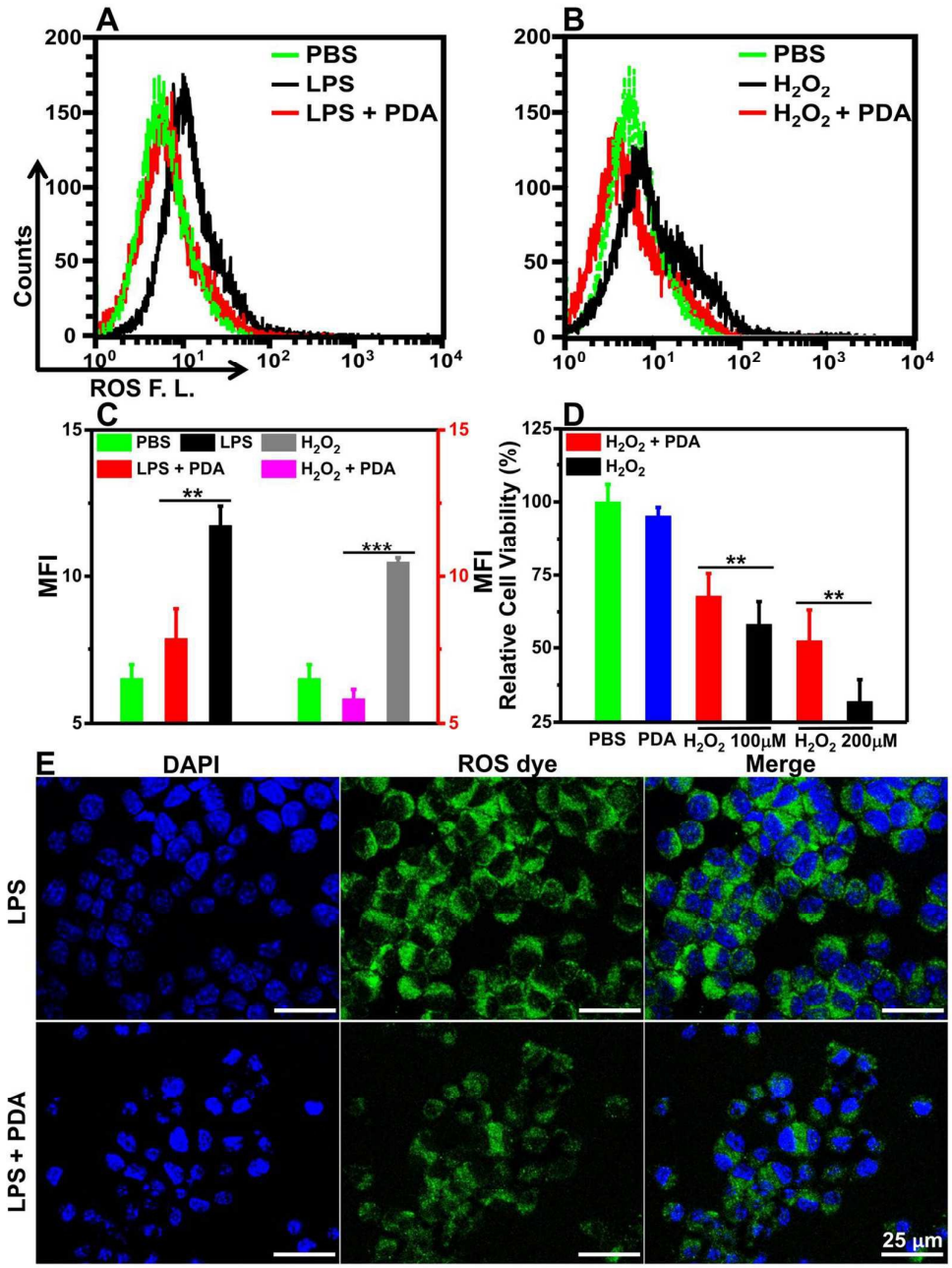

Figure 2. In vitro antioxidant and anti-inflammatory experiments. (A&B) Intracellular ROS scavenging by PDA in LPS-treated (A) or H_2O_2-treated (B) Raw 264.7 cells as detected by the flow cytometer using DCFH-DA as the ROS-specific probe. (C) Mean fluorescence intensity (MFI) calculated based on the flow cytometer data in (A&B). (D) The relative viabilities of Raw 264.7 cells incubated with H_2O_2 (200 μM and 100 μM) with or without PDA (80 μg/ml). ** $p < 0.01$, *** $p < 0.001$. (E) Confocal fluorescence images of ROS levels in the LPS-treated cells with or without PDA treatment using DCFH-DA as the ROS probe. Scale bar = 25 μm.

View Article Online
DOI: 10.1039/C8NR00838H

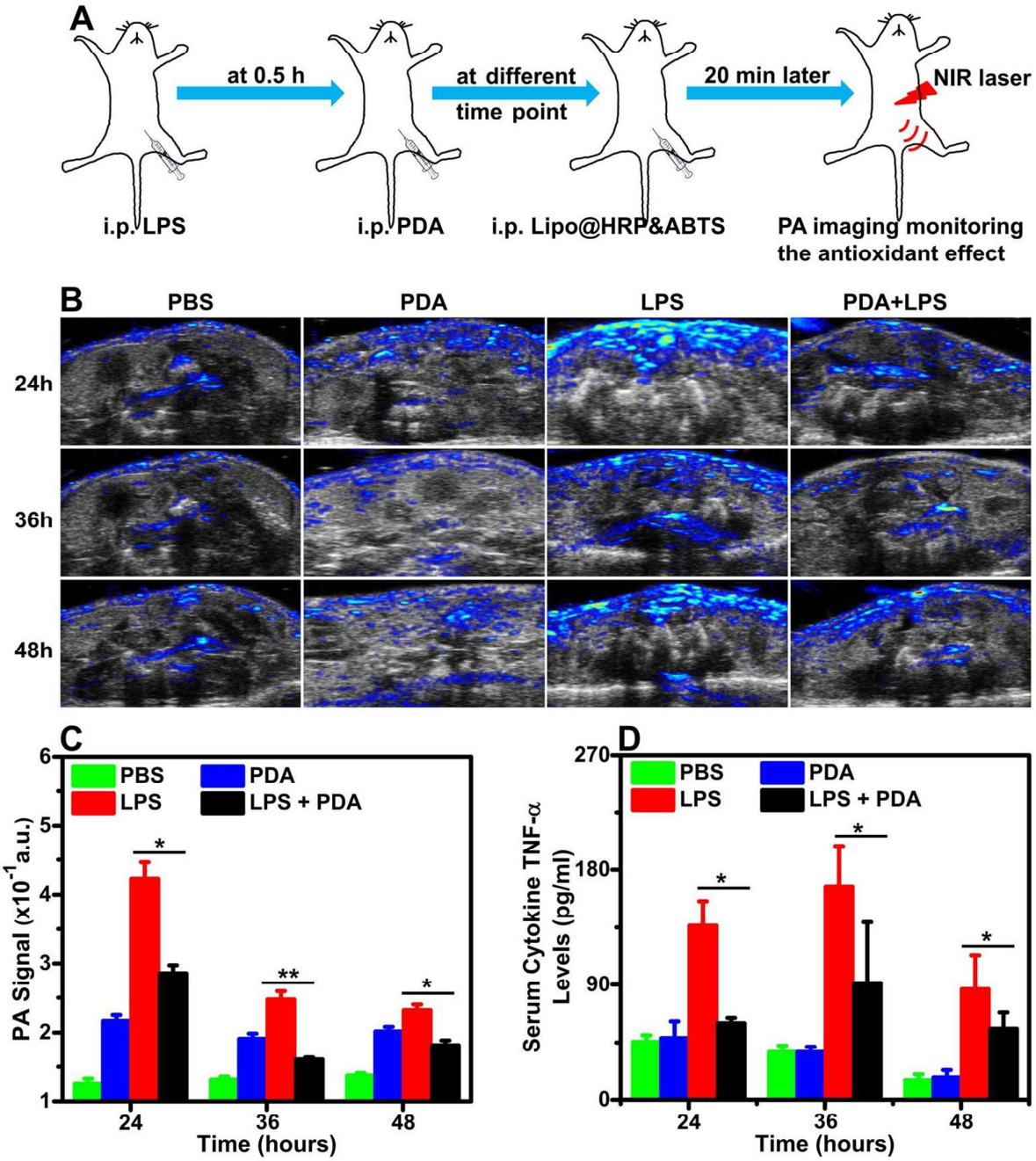

Figure 3. In vivo PA imaging to monitor relief of acute peritonitis by PDA treatment. (A) Schematic illustration showing the experimental design. LPS was i.p. injected into mice to induce acute peritonitis, which was ameliorated by PDA. The therapeutic effect could be monitored by PA imaging for in vivo H_2O_2 detection. (B) In vivo PA images of mouse abdomen at different time points (24 h, 36 h and 48 h) post injection of LPS with or without i.p. injection of PDA. (C) PA signals at 780 nm for mouse abdomen of all groups based on PA imaging data in (B). (D) Serum cytokine TNF-α from mice evaluated at 24 h, 36 h and 48 h post injection of LPS. * $p < 0.05$ and ** $p < 0.01$.

View Article Online
DOI: 10.1039/C8NR00838H

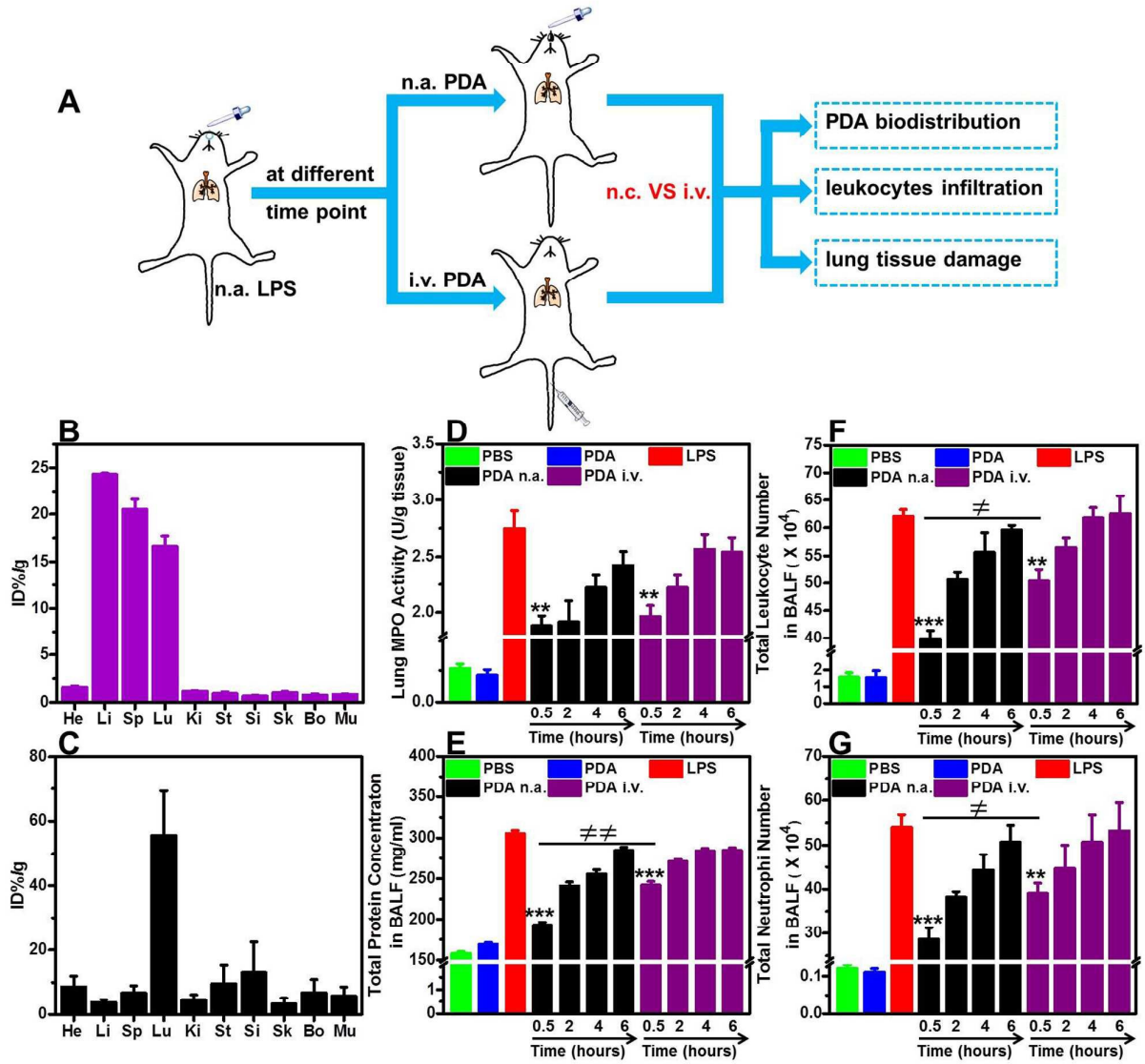

Figure 4. PDA injection with different administration routes for in vivo ALI treatment. (A) Schematic illustration showing the establishing process of the ALI model and the two treatment routes. (B&C) The biodistribution of PDA by i.v. injection (B) or n.a. dripping (C) at 24 h post treatment. He: heart; Li: liver; Sp: spleen; Lu: lung; Ki: kidney; St: stomach; Si: small intestine; Sk: skin; Bo: bone; Mu: muscle. (D-G) Comparison of therapeutic responses between i.v. injection and n.a. administration of PDA evaluated at different intervention time points (0.5 h, 2 h, 4 h and 6 h) post model establishment, including the lung MPO activity (D), the total protein concentration (E), the total leukocyte number (F), and the total neutrophil number (G). P values were calculated by the Student's t-test. ≠ $p < 0.05$, ≠≠ $p < 0.01$ means n.a. administration group versus i.v. injection group. ** $p < 0.01$, ** $p < 0.001$ versus LPS group.

View Article Online
DOI: 10.1039/C8NR00838H

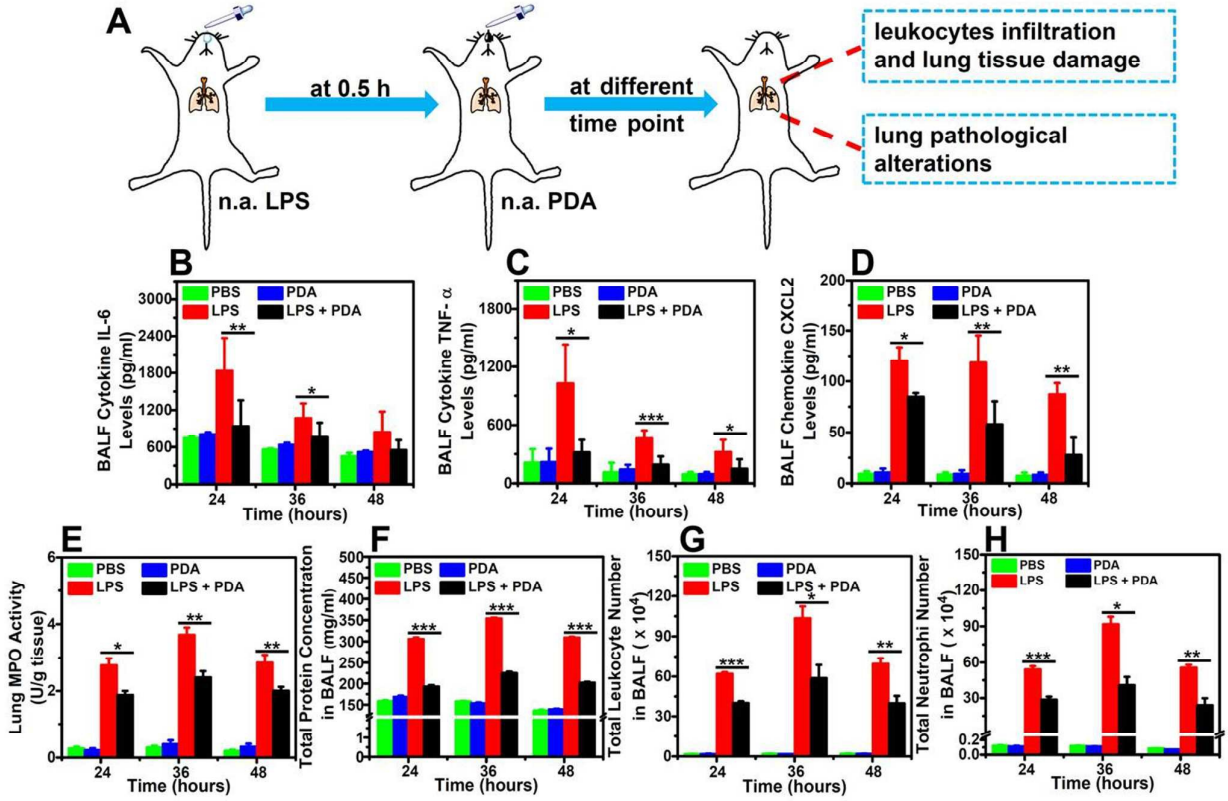

Figure 5. In vivo therapy with PDA for ALI treatment. (A) Schematic illustration showing the ameliorative process of ALI induced by PDA. (B - D) BALF cytokines including IL-6, TNF-α, and CXCL2 from mice measured at 24 h, 36 h and 48 h post dripping of LPS. (E-H) The assessment in lung MPO activity (E), the BALF total protein concentration (F), the BALF total leukocyte number (G), and the BALF total neutrophil number (H) at different time point (24 h, 36 h and 48 h) after LPS inhalation. * $p < 0.05$, ** $p < 0.01$ and *** $p < 0.001$.

View Article Online
DOI: 10.1039/C8NR00838H

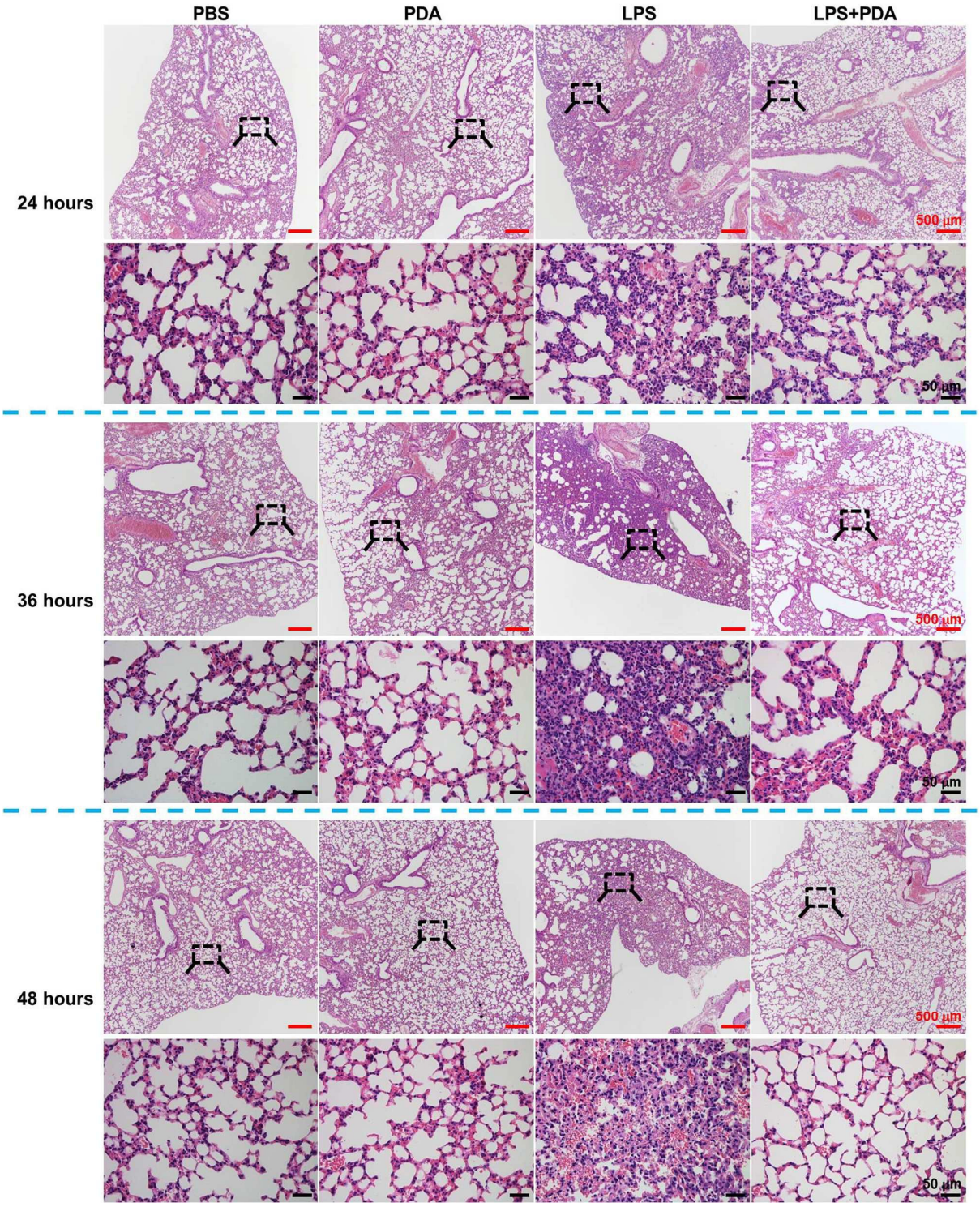

Figure 6. In vivo lung histological examination. H&E stained images of the lung tissues collected from all groups. Scale bar (red line) = 500 μm; Scale bar (black line) = 50 μm.